Proceedings of the 11th ICPMG 2026
11th International Conference on Physical Modelling in Geotechnics
8-12 June 2026, Zurich, Switzerland

Modeling installation and pullout response of snakeskin-textured piles

L. Sekulic, D.A. Dao, D. Alkateeb, J. Grabe
Hamburg University of Technology, Germany, lennart.sekulic@tuhh.de, duy.anh.dao@tuhh.de, diaa.alketeeb@tuhh.de, grabe@tuhh.de

A. Martinez
University of California Davis, USA, amart@ucdavis.edu

ABSTRACT: Applying snake-textured surface to piles enables a direction-dependent interface strength. The positive effect of this texture on increasing interface strength during pullout has been demonstrated in centrifuge and field tests. However, these tests are costly, limit the ability to explore a wider range of influencing parameters, and do not offer information on soil response at the element level. To overcome this limitation, numerical simulations offer a valuable extension. Currently, few numerical models piles exist that can enable systematic variation of design parameters beyond physical testing. This study addresses this gap by developing and validating a numerical model for snake-textured piles during installation and pullout. The Coupled Eulerian-Lagrangian (CEL) method, which accounts for large deformations, was used to model snakeskin-inspired piles, and the results were compared with centrifuge test results at prototype scales. The pile was modelled as a rigid steel element with Lagrangian discretization, while the soil, Ottawa F65 sand, was represented with Eulerian elements using a hypoplastic constitutive model with intergranular strains. Both installation and pullout processes were simulated. The numerical results show good agreement with the centrifuge data, with a mean absolute percentage error of 9.7% regarding base pressure. The developed model accurately reproduces centrifuge test behavior and provides a basis for extended parametric studies with more detailed measurements beyond the scope of physical experiments.

1 INTRODUCTION

Direction-dependent interface behavior offers new opportunities for optimizing pile foundations. Inspired by biological systems, several studies have explored textured surfaces that create anisotropic frictional behavior. Snakeskin is a well-studied example: the ventral scales of snakes generate lower friction when moving forward and higher friction when retracting (Gray and Lissmann 1950; Marvi and Hu 2012). Laboratory tests have shown that such directional effects can be transferred to engineered surfaces. Interface shear tests on snakeskin-inspired textures demonstrated higher strength and dilatancy in the cranial direction (i.e., soil against scales) compared to the caudal direction (i.e., soil along scales) (Martinez et al. 2019; Stutz and Martinez 2021; O'Hara and Martinez 2020; Huang and Martinez 2021). Centrifuge and field load tests on piles and soil anchors with snake-textured surfaces confirmed greater shaft resistance in the cranial direction during both installation and pullout (Martinez and O'Hara 2021; Martinez et al. 2024), while discrete element simulations provide consistent trends and data on particle level (Zhong et al. 2021).

Although experiments yield valuable insights, they are limited by cost and experimental constraints that restrict systematic variation in texture geometry and loading conditions and do not capture soil response information at the element scale. Numerical modeling can address these limitations. However, few validated numerical frameworks currently exist that can reproduce the installation and pullout responses of snake-textured piles. The objective of this study is to develop and validate a numerical model capable of capturing the behavior of snake-textured piles during installation and pullout. Centrifuge tests were simulated at prototype scale using the Coupled Eulerian–Lagrangian (CEL) method to account for large soil deformations.

2 CENTRIFUGE TESTS

O'Hara and Martinez (2022) conducted a series of centrifuge tests to investigate the load transfer mechanisms of snake-textured and reference smooth and rough piles during installation and pullout in sand. The experiments were performed at the University of California Davis Center for Geotechnical Modeling on the 9-m-radius centrifuge at an acceleration of 30*g*. Air-pluviated Ottawa F65 sand was used as the test material at a relative density of approximately 65%. The aluminum model piles had a total length of 420 mm, outer diameter, B_{pile}, of 19.05 mm, and an average wall thickness of 3.05 mm, and were instrumented with internal strain gauges to record axial force distributions along the pile shaft. The test series examined the influence of surface texture orientation, asperity geometry, and embedment depth on the direction-dependent shaft resistance.

Figure 1 shows the smooth reference pile test, DI-RP-0.30, in the test environment that was selected for numerical simulation. The model pile had surface asperities with a length, L, of 12 mm and a height, H, of 0.30 mm. The pile was installed by quasi-static in-flight displacement-controlled pushing to a target embedment depth of 9*D*. Following installation, monotonic pullout loading was applied at a constant displacement rate. The critical state interface friction angle of the pile material, δ'_{cs}, determined from laboratory testing on planar surfaces with the same material as the piles and Ottawa F65 sand (Palumbo 2018), was determined as 19.0° in both shearing directions. The following comparison focuses on the load–displacement behavior during installation and pullout.

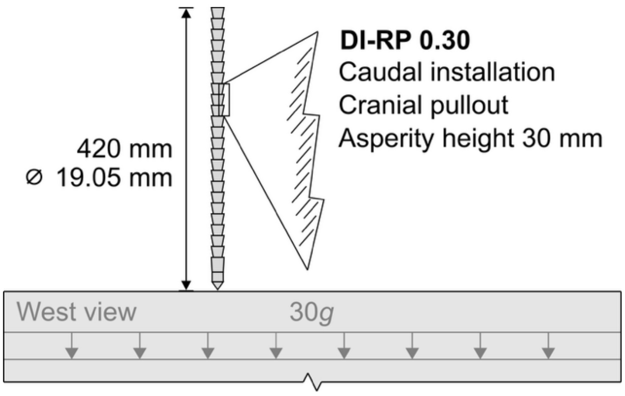

Figure 1: Chosen pile from centrifuge tests by O'Hara and Martinez (2022) for numerical model

3 NUMERICAL MODELING

Large soil deformations were modeled using the Coupled Eulerian–Lagrangian (CEL) formulation implemented in Abaqus/Explicit. In a purely Lagrangian description, the mesh follows the material, allowing accurate tracking of interfaces but leading to severe element distortion at large strains. In contrast, the Eulerian description keeps the mesh fixed while material flows through it, represented by the Eulerian Volume Fraction (EVF), but may introduce numerical diffusion.

The CEL approach combines both advantages: the pile is discretized with Lagrangian elements, while the surrounding soil and the overlying void space are represented using Eulerian elements. Interaction between the two domains is handled through the built-in Eulerian–Lagrangian contact algorithm with automatic contact detection, and material transport is performed via a remapping step (Dassault Systèmes, 2016; Noh, 1963; Benson, 1992).

The method is well established for geotechnical problems involving large deformations (e.g., Dao et al., 2023, 2025; Bienen et al., 2021). Time integration is carried out using an explicit central-difference scheme, which updates the state variables from the previous increment without global iterations, allowing efficient treatment of contact and advection. Numerical stability is controlled by a critical time increment that depends on the smallest element dimension and the local dilational wave speed of the material, which may require small time steps near refined contact regions.

3.1 Constitutive model

The soil behavior was modeled using the hypoplastic constitutive law of Wolffersdorff (1996) combined with the intergranular strain extension of Niemunis and Herle (1997) to represent small-strain stiffness, as well as unloading and reloading due to the bio-inspired texture. The model relates the stress rate to the strain rate through a non-linear tensor function:

$$\dot{\mathrm{T}} = \mathbf{M}(\mathbf{T}, e) : \mathbf{D} \qquad (1)$$

where $\dot{\mathbf{T}}$ is the effective stress rate tensor, $\mathbf{D}$ is the strain-rate tensor, and $\mathbf{M}$ is a fourth-order tensor that depends on the current effective Cauchy stress $\mathbf{T}$ and the void ratio e The limits of the void ratio for the loosest, critical, and densest states (e_{i}, e_{c}, and e_{d}) vary with the mean effective stress, $p' = (1/3)\ \mathrm{tr}(\mathbf{T})$, according to Bauer (1996):

$$\frac{e_{\mathrm{i}}}{e_{\mathrm{i0}}} = \frac{e_{\mathrm{c}}}{e_{\mathrm{c0}}} = \frac{e_{\mathrm{d}}}{e_{\mathrm{d0}}} = \exp\left[\left(-\frac{\mathrm{tr}(\mathbf{T})}{h_{\mathrm{s}}}\right)^{n}\right] \qquad (2)$$

where h_{s} is the granular hardness and n is an exponent obtained from oedometer tests. Base parameters for the hypoplastic model for Ottawa F65 sand, characterized by a critical state friction angle of 29.6° and a density of 1665.6 kg/m³, were taken from Liao et al. (2023). The parameters were then recalibrated for the cone penetration tests conducted by O'Hara and Martinez (2022) as presented in Table 1, and then used in the soil-structure interaction simulations.

3.2 Numerical model

Figure 2 presents the model setup, where the pile was modeled as a rigid Lagrangian body controlled by a reference point located at the pile tip, with prototype dimensions from O'Hara and Martinez (2022). The soil domain and an overlying 1 m void layer were discretized by Eulerian elements to accommodate large deformations and potential material heave.

Given the inherent symmetry of the model, only one quarter of the model cross-section was simulated. The soil domain consisted of a one-fourth vertical cylinder with a depth of 15 m. The pile shaft was represented by 25 stacked truncated cones, each 0.36 m in height, creating a slight taper from a lower radius of 0.277 m to an upper radius of 0.286 m. The pile tip was modelled as a cone with a 60° apex angle, as shown in Figure 2.

Base parameters for the soil were adopted from Liao (2023) and were recalibrated by adjusting them within common ranges to match the conducted CPT results with plane-strain FE simulations of CPT, following the procedure proposed by Alkateeb and Grabe (2025) and Alkateeb et al. (2026), resulting in the parameters summarized in Table 1. The relative density of 65% from the centrifuge tests corresponds to a void ratio of 0.604.

General contact in Abaqus was employed to simulate pile-soil interaction. The friction coefficient was according to O'hara and Martinez (2022) 19°, which corresponds to tan $\delta = 0.344$.

The pile mesh contained approximately 5.8×10^3 Lagrangian elements, and the soil domain contained about 103.5×10^3 Eulerian elements, refined near the pile-soil interface. The mesh size is presented in Figure 3 and was selected based on a sensitivity study, Symmetry planes constrained motion normal to their surfaces, while the base and outer boundaries prevented normal movement of the Lagrangian domain.

Table 1: Calibrated hypoplastic parameters of Ottawa sand

φ_c	h_s	n	e_{d0}	e_{c0}	e_{i0}	α	β	m_T	m_R	R_{max}	β_χ	χ
29.6 °	3.5×10^6 kPa	0.31	0.51	0.78	0.896	0.25	2	2	5	10^{-4}	0.5	1

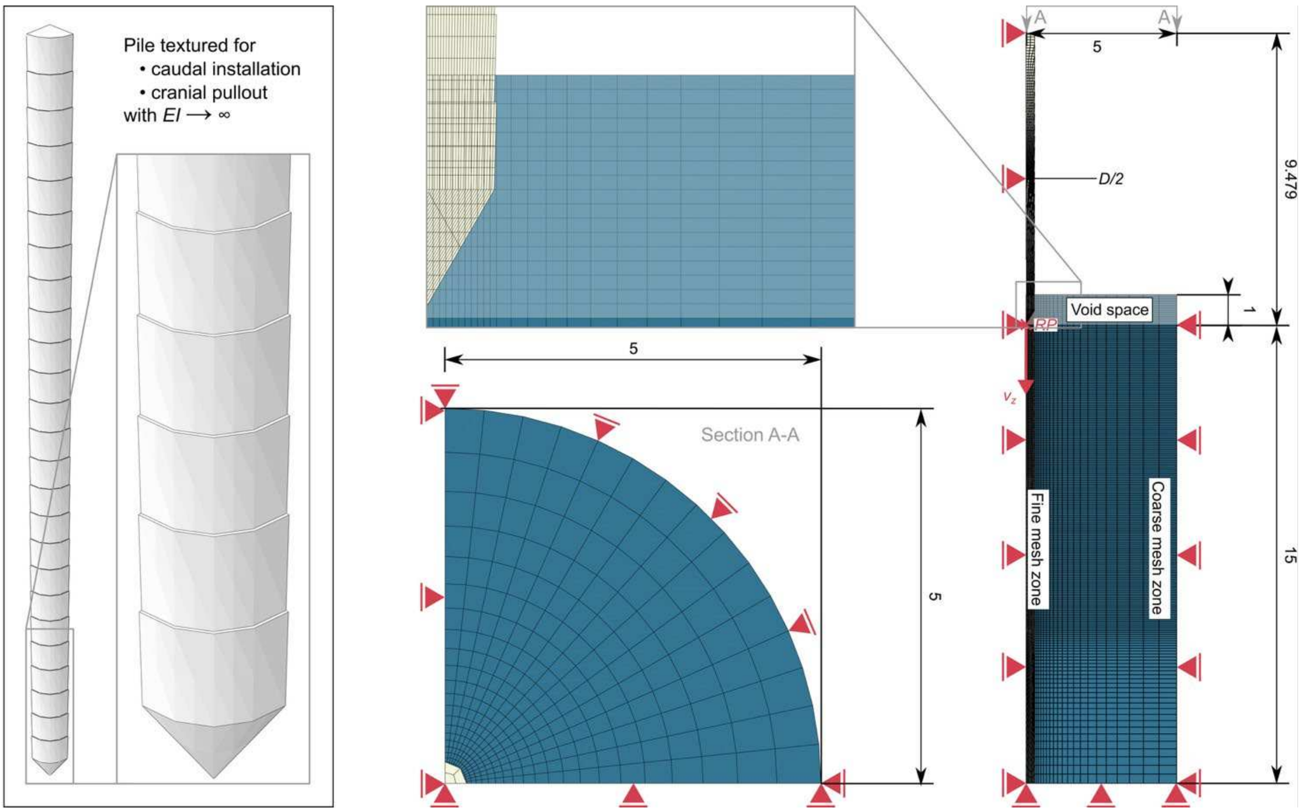

Figure 2: Numerical model for installation and pulling out of textured pile

3.3 Loading steps

The loading sequence consisted of three steps:

1) Initialization: Boundary conditions were activated, and the K_0 stress state was established, using $K_0 = 1 - \sin \varphi_c = 1 - \sin 29.6\,° = 0.506$.
2) Installation: A constant downward velocity of 1 m/s was applied at the pile-head reference point for 7.5 s, corresponding to a penetration depth of 7.5 m.
3) Pull-out: The pile was subsequently extracted by imposing an upward velocity of 1 m/s at the reference point for 0.1 s.

3.4 Mesh Sensitivity

The accuracy of the simulations is assessed with the mean absolute percentage error (MAPE) for the base pressure during installation. For each data point, the absolute difference between the predicted and measured values are taken, expressed as a percentage of the measured value, and then averaged across all observations. A low MAPE denotes a good agreement.

Figure 3 presents the results of the mesh sensitivity study for the soil domain. The MAPE decreases slightly starting from 4.6 × 10^4 soil elements. To balance computational efficiency and accuracy, a mesh consisting of 10.4 × 10^4 elements was adopted for subsequent analyses.

4 RESULTS AND DISCUSSION

Figure 4 shows the base pressure with depth during pile installation and Figure 5 presents the pile head load with depth during pile installation and pullout. The simulation achieves a MAPE of 9.7% and 35.6% for base resistance and head load, respectively, indicating close agreement with the experimental results and providing a reliable basis for further analysis.

Figure 6 and Figure 7 present horizontal stress and void ratio distributions at representative stages during the simulation. Immediately after stress initialization (1), the horizontal stresses follow the prescribed linear increase with depth, and the void ratio displays the input across the entire soil domain, with a slightly looser state, approximately 1% higher, resulting from minor numerical smearing with the upper void space during initialization.

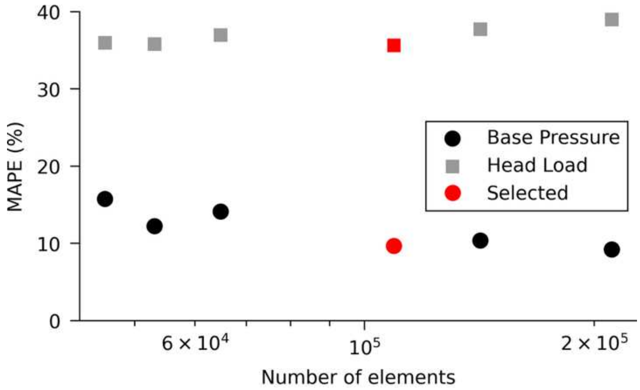

Figure 3: Soil mesh sensitivity

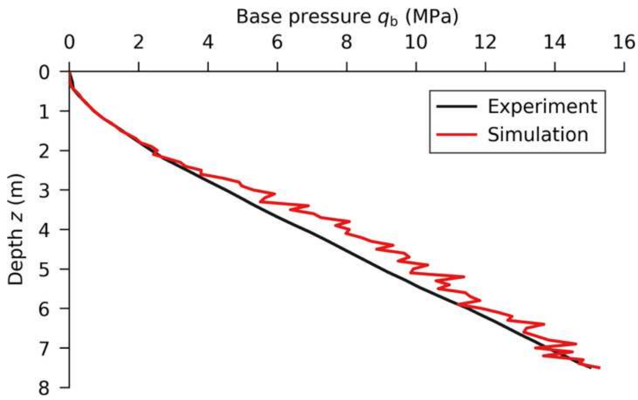

Figure 4: Comparison of base pressure of simulation and centrifuge experiment

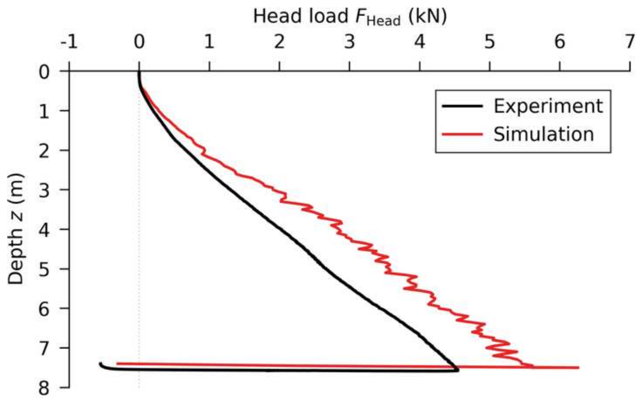

Figure 5: Comparison of pile head load of simulation and centrifuge experiment

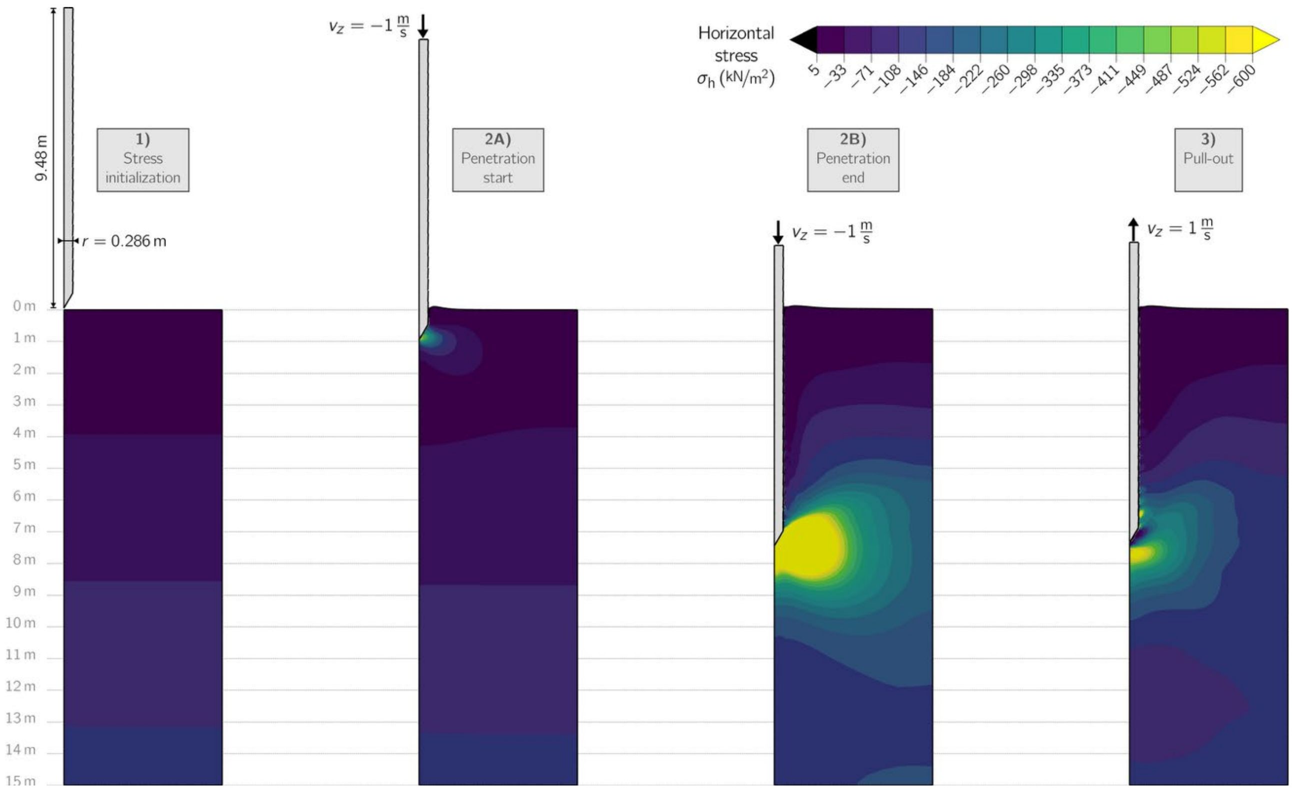

Figure 6: Simulated horizontal stress distribution due to pile installation and extraction

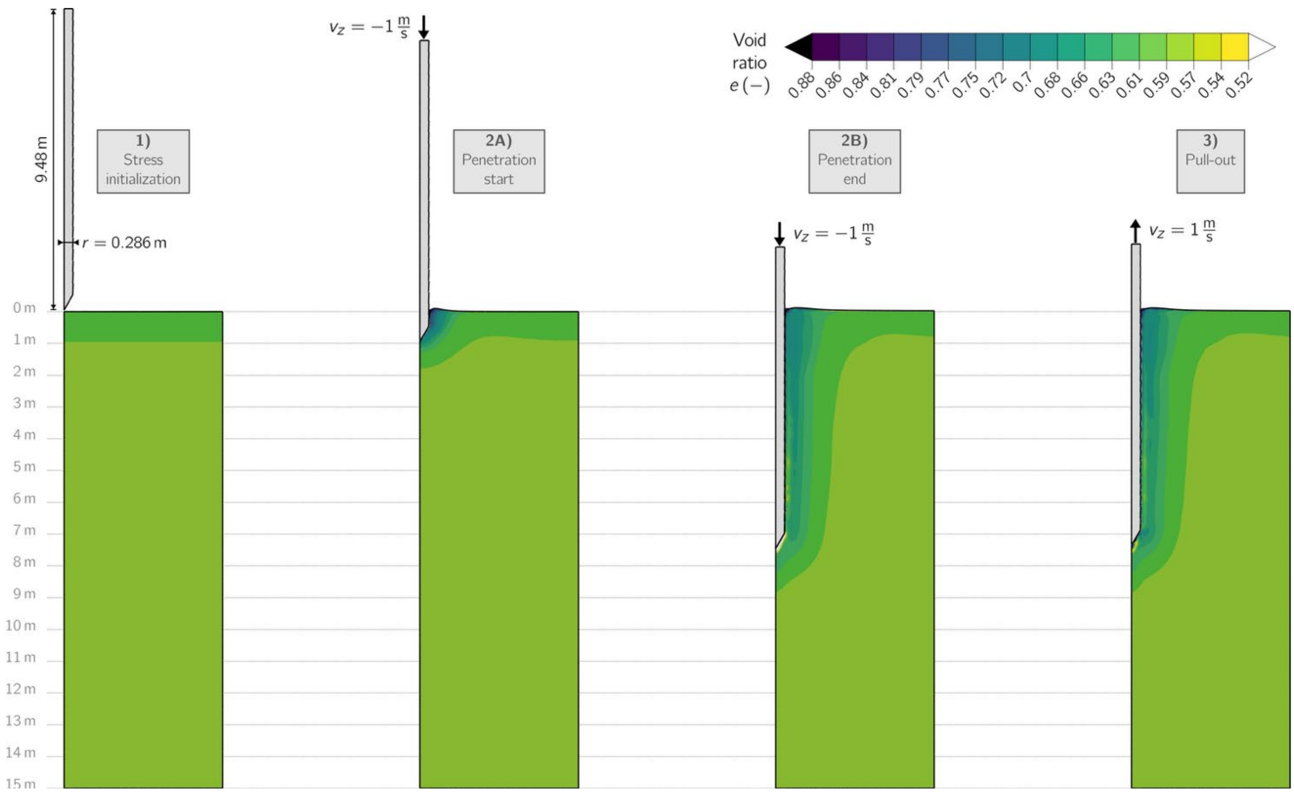

Figure 7: Simulated void ratio distribution due to pile installation and extraction

Upon initial contact between the pile and the soil (2A), a bulb with increased stress begins to develop around the pile tip. The void ratio distribution remains largely uniform, with localized dilation within the developing failure mechanism around the pile tip and along the upper shaft, in correspondence with the stress increase. Beneath this area, a slightly denser region forms, corresponding to compression of the soil displaced downward by the advancing pile.

As penetration progresses to the final embedment depth of 7.5 m, the stress bulb continues to expand (2B). A continuous band of loose soil develops along the pile shaft and ahead of the tip. At the pile head, the soil densifies locally. At the pile-soil interface, a very narrow zone of soil with the maximum void ratio develops, marking shear band with strongest dilation. Adjacent to this zone, thin bands of low void ratio can be observed around the textured scales, as shown in Figure 8, suggesting an increase in resistance with densification due to interlocking and particle rearrangement.

At the end of pile pullout (Δz = 0.1 m), a rapid unloading occurs, resulting in a marked reduction in horizontal stress near the pile tip (3). The previously loosened zone around the shaft remains, indicating continued dilation along the contact interface. Below the pile tip, the void ratio is lower, corresponding to the compressed soil mass formed during penetration. Localized regions of slightly reduced void ratio also appear along the shaft, reflecting minor densification associated with upward soil movement.

Overall, the numerical simulation not only reproduces the global load-displacement behavior observed in centrifuge tests but also enables direct observation of the meso-scale soil response that is experimentally inaccessible. The stress and void ratio fields reveal how localized dilation and densification evolve around textured pile surfaces, revealing the mechanisms by which surface roughness and interlocking influence pile resistance.

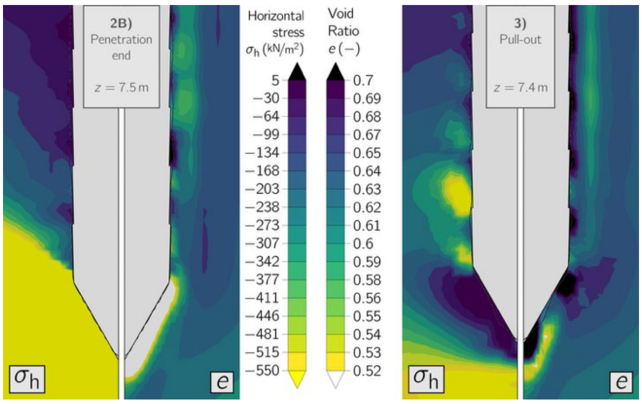

Figure 8: Stress and void ratio distribution around the scales

5 CONCLUSIONS

A numerical model was developed using the CEL method to simulate both the penetration and extraction of a snakeskin-inspired pile installed in a caudal direction and pulled out cranially in prototype size. This model was used to recreate a centrifuge test that was previously performed in medium dense Ottawa F65 sand. The resulting stress and void ratio contours were found to be physically consistent. Furthermore, comparison between simulated and measured responses yielded a MAPE of 9.7% for the base pressure and 35.6% for the head load, indicating close agreement. The validated model provides a reliable basis for extending the analysis to additional geometric variations, thereby enabling additional investigation of the load-displacement behavior without the need for further resource-intensive physical testing.

ACKNOWLEDGEMENTS

The authors are grateful for the financial support provided by German Research Foundation (DFG) supporting this project under Grant number GT 1024/61-1

REFERENCES

Alkateeb D. and Grabe J. (2025). Bearing capacity of tension steel piles in thinly inter-layered soils: numerical class-A prediction vs. field measurements. *International Journal for Numerical and Analytical Methods in Geomechanics*. https://doi.org/10.1002/nag.70132

Alkateeb, D., Dao, D. A., Schröder, M. and Grabe, J. (2026). CPT-based FEM prediction of pile under monotonic and high-cyclic lateral loading in sand. *Submitted*

Bauer, E. (1996). Calibration of a comprehensive hypoplastic model for granular materials. *Soils and foundations*, 36(1): 13-26. https://doi.org/10.3208/sandf.36.13

Bienen, B., Fan, S., Schröder, M. and Randolph, M. F. (2021). Effect of the installation process on monopile lateral response. *Proceedings of the Institution of Civil Engineers-Geotechnical Engineering*, 174(5): 530–548 https://doi.org/10.1680/jgeen.20.00219

Benson, D. J. (1992). Computational methods in Lagrangian and Eulerian hydrocodes. *Computational Methods in Applied and Mechanical Engineering*, 99 (2): 235–394. https://doi.org/10.1016/0045-7825(92)90042-I

Dassault Systèmes (2025). ABAQUS Analysis User's Manual. Available with the ABAQUS software documentation.

Dao, D. A., Tafili, M., Williams-Riquer, F., Grabe, J. and Wichtmann, T. (2025). Large deformation simulations of structure–soil-interaction in anisotropic fine-grained soils. *Computers and Geotechnics*, 188: 107537. https://doi.org/10.1016/j.compgeo.2025.107537

Dao, D. A., Alkateeb, D. and Schröder, M. (2023). Discrepancies between element tests and large-scale LDFE simulations: A case study on anchor kinematics during installation in clay. *Computers and* *geotechnics*, 163: 105698. https://doi.org/10.1016/j.compgeo.2023.105698

Gray, J. and Lissmann, H. W. (1950). The kinetics of locomotion of the grass-snake. *Journal of Experimental Biology*, 26(4): 354-367. https://doi.org/10.1242/jeb.26.4.354

Huang, L. and Martinez, A. (2021). Load transfer anisotropy at snakeskin-inspired clay-structure interfaces. *Proceedings of the International Foundations Congress and Equipment Expo 2021*, pp. 119-129. https://doi.org/10.1061/9780784483428.013

Liao, D., Yang, Z. X., Wang, S. and Wu, W. (2023). A hypoplastic model for cemented sand under monotonic and cyclic loading. *Canadian Geotechnical Journal*, 61(5): 915-930. https://doi.org/10.1139/cgj-2023-0079

Martinez, A., Palumbo, S. and Todd, B. D. (2019). Bioinspiration for anisotropic load transfer at soil–structure interfaces. *Journal of Geotechnical and Geoenvironmental Engineering*, 145(10): 04019074. https://doi.org/10.1061/(ASCE)GT.1943-5606.0002138

Martinez, A. and O'Hara, K. B. (2021). Skin friction directionality in monotonically-and cyclically-loaded bio-inspired piles in sand. *The Journal of the Deep Foundations Institute*, 15(1): 1-15.

Martinez, A., Zamora, F. and Wilson, D. (2024). Field evaluation of the installation and pullout of snakeskin-inspired anchorage elements. *Journal of Geotechnical and Geoenvironmental Engineering*, 150(8): 04024068-1 - 04024068-17. https://doi.org/10.1061/JGGEFK.GTENG-12311

Marvi, H. and Hu, D. L. (2012). Friction enhancement in concertina locomotion of snakes. *Journal of the Royal Society Interface*, 9(76): 3067-3080.

Noh, W. (1963). CEL: A Time-Dependent, Two-Space-Dimensional, Coupled Eulerian-Lagrange Code. Lawrence Radiation Laboratory.

O'Hara, K. B. and Martinez, A. (2020). Monotonic and cyclic frictional resistance directionality in snakeskin-inspired surfaces and piles. *Journal of Geotechnical and Geoenvironmental Engineering*, 146(11): 04020116. https://doi.org/10.1061/(ASCE)GT.1943-5606.0002368

O'Hara, K. B. and Martinez, A. (2022). Load transfer directionality of snakeskin-inspired piles during installation and pullout in sands. *Journal of Geotechnical and Geoenvironmental Engineering*, 148(12): 04022110. https://doi.org/10.1061/(ASCE)GT.1943-5606.0002929

Palumbo, S. (2018). *Anisotropic interface shear behavior of granular soil and surfaces biologically-inspired by snakeskin*. Master's dissertation, Department of Civil and Environmental Engineering, University of California

Stutz, H. H. and Martinez, A. (2021). Directionally dependent strength and dilatancy behavior of soil–structure interfaces. *Acta Geotechnica*, 16(9): 2805-2820. https://doi.org/10.1007/s11440-021-01199-5

von Wolffersdorff, P. (1996). A hypoplastic relation for granular materials with a predefined limit state surface. *Mechanics of Cohesive-frictional Materials*, 1(3): 251–271. https://doi.org/10.1002/(SICI)1099-1484(199607)1:3<251::AID-CFM13>3.0.CO;2-3

Niemunis, A. and Herle, I. (1997). Hypoplastic model for cohesionless soils with elastic strain range. *Mechanics of Cohesive-frictional Materials*, 2(4): 279–299. https://doi.org/10.1002/(SICI)1099-1484(199710)2:4<279::AID-CFM29>3.0.CO;2-8

Zhong, W., Liu, H., Wang, Q., Zhang, W., Li, Y., Ding, X. and Chen, L. (2021). Investigation of the penetration characteristics of snake skin-inspired pile using DEM. *Acta Geotechnica*, 16(6): 1849-1865. https://doi.org/10.1007/s11440-020-01132-2